A Potential BNCT Agent Selectively Suppresses High-Grade Glioma: In Vitro and In Vivo Exploration

Catalina Alamón[a,b,†], Belén Dávila[a,†], María Fernanda García[c], Susana Nievas[d], María Alejandra Dagrosa[e], Silvia Thorp[f], Mariángeles Kovacs[b], Emiliano Trias[b], Ricardo Faccio[g], Martín Gabay[h], Nidal Zeineh[h], Abraham Weizman[h], Francesc Teixidor[i], Clara Viñas[i], Moshe Gavish[h,*], Hugo Cerecetto[a,c,*], Marcos Couto[a,*]

[a] Grupo de Química Orgánica Medicinal, Instituto de Química Biológica, Facultad de Ciencias, Universidad de la República, Montevideo 11400, Uruguay. [b] Laboratorio de Neurodegeneración, Institut Pasteur de Montevideo, Montevideo 11400, Uruguay. [c] Área de Radiofarmacia, Centro de Investigaciones Nucleares, Facultad de Ciencias, Universidad de la República, Montevideo 11400, Uruguay. [d] Department of Boron Neutron Capture Therapy, [e] Department of Radiobiology, and [f] Department of Instrumentation and Control, National Atomic Energy Commission, Buenos Aires C1429BNP, Argentina. [g] Área Física, DETEMA, Facultad de Química, Universidad de la República, Montevideo 11800, Uruguay. [h] Molecular Pharmacology, Faculty of Medicine, Technion Institute of Technology, Haifa 3200003, Israel. [i] Institut de Ciències dels Materials de Barcelona-CSIC, Campus UAB, Bellaterra 08193, Spain.

KEYWORDS epidermal growth factor receptors, glioblastoma, boron neutron capture therapy.

ABSTRACT: Glioblastoma (GBM), as the most CNS intractable disease, has spoiled millions of lives due to its high mortality. Even though several efforts have been done, the existing treatments have had limited success. In this sense, we studied a lead compound, the boron-rich selective EGFR-inhibitor hybrid **1**, as a potential drug for GBM treatment. For this end, we analyzed the *in vitro* activity of hybrid **1** in a glioma/primary astrocytes co-culture, studying cellular death types triggered by treatment with this compound and its cellular localizations. Additionally, hybrid **1** concentrated boron in glioma cells selectively and more effectively than the BNCT-clinical agent ^{10}B-L-boronophenylalanine and thus displayed better *in vitro*-BNCT effect. This encouraged us to analyze hybrid **1** *in vivo*. Therefore, immunosuppressed mice bearing U87 MG human GBM were treated with both **1**- and **1**–encapsulated in a modified liposome (recognized by brain blood barrier peptide transporters) observing a potent *in vivo per se* antitumor activity (tumor size decrease and animal survival increase). These data demonstrate that **1** could be a promising new targeted therapy for GBM.

■ INTRODUCTION

Among infiltrative gliomas, glioblastoma (GBM, previously known as glioblastoma multiforme) is considered the most devastating and most frequent primary intraparenchymal brain tumor with a median survival of generally less than 15 months from the time of diagnosis.[1] Despite intense efforts, challenges still arise as the therapeutic options available, including tumor resection, followed by a combination of radiation and chemotherapy (typically using temozolomide, **TMZ**, Figure 1) do not improve the prognosis significantly.[2] In this regard, improvement of treatment options for patients with GBM is an unmet need. Targeted small molecules therapy toward tyrosine kinase receptors (TKR) is gaining increasing interest and acceptance to treat GBM.[3-6] Among them, erlotinib (**Erl**, Figure 1), is an oral small molecule that has been extensively studied in preclinical and clinical trials of GBM.[7,8] The best results were achieved when **Erl** was combined with other drugs, i.e. **TMZ**, and radiotherapy, suggesting that **Erl** may be beneficial when combined with other treatments, rather than as a monotherapy.[7,9,10] On the other hand, another approach that offers therapeutic opportunities for GBM is the boron neutron capture therapy (BNCT) which is based on the nuclear capture and fission reactions [^{10}B(1n,α)^{7}Li] that occur when the stable ^{10}B is irradiated with neutrons generating high linear energy transfer alpha particles (stripped down helium nuclei, $^{4}He^{2+}$, 150 keV μm^{-1}) and recoiling lithium cations ($^{7}Li^{3+}$, 175 keV μm^{-1}).[11,12] Due to these particles having a linear path trajectory similar to the diameter of a cell (5–9 μm), the irradiation damage can affect only those cells containing sufficient amounts of boron and spare adjacent normal cells. The most extensively evaluated agents for BNCT are (L)-4-dihydroxyborylphenylalanine, known as boronophenylalanine or **BPA** (Figure 1), commonly administrated intravenously as a **BPA** fructose adduct (**BPA-f**), and disodium mercaptoundecahydro-*closo*-dodecaborate ($Na_2B_{12}H_{11}SH$), commonly known as sodium borocaptate or **BSH** (Figure 1). Nevertheless, the major problem with both **BSH** and **BPA-f** is the significant variability in tumor uptake, especially in brain tumors. This was plainly confirmed by Goodman *et al.* in a biodistribution and pharmacokinetic study involving nearly 20 patients with high-grade gliomas.[13] Taking this background as a starting point, we recently reported a broad range of new hybrid compounds bearing boron-rich carboranyl clusters and the anilinoquinazoline-framework from **Erl**, to be applied as bimodal therapeutic agents.[14,15] Among them, a lead compound, i.e. hybrid **1** (Figure 1), was selected due to its excel-

lent drug-like properties,[16] including EGFR-inhibition ability against wild type and T790M mutant EGFR (IC_{50} of 2.3 and 1100 nM, respectively),[15] selectivity towards tumor cells, absence of mutagenicity and acute oral toxicity.[17]

Herein, we report the performed studies to explore the pharmacological potential of the hybrid **1**: i) Firstly, as to resemble the cellular environment of a developing brain tumor, hybrid **1** effects and death-mechanisms were studied on U87 MG cells co-cultured with primary astrocytes using confocal microscopy and flow cytometry; ii) Secondly, U87 MG cellular localization with time of compound **1** was analyzed by B-Raman microscopy; iii) Thirdly, to determine whether our *in vitro* findings would translate into anti-glioma effect *in vivo*, anti-cancer activity using an experimental U87 MG-glioma mouse model, was determined by intraperitoneal administration of hybrid **1** in DMSO or in a modified liposome, which is able to be recognized by blood brain barrier (BBB) peptide transporters; iv) Fourth, intracellular boron uptake was quantitatively measured on glioma cells and astrocytes by inductively-coupled plasma optical emission spectrometry; v) Fifthly, BNCT-efficacy studies of hybrid **1** were performed on glioma cells as *in vitro* proof-of-concept assay.

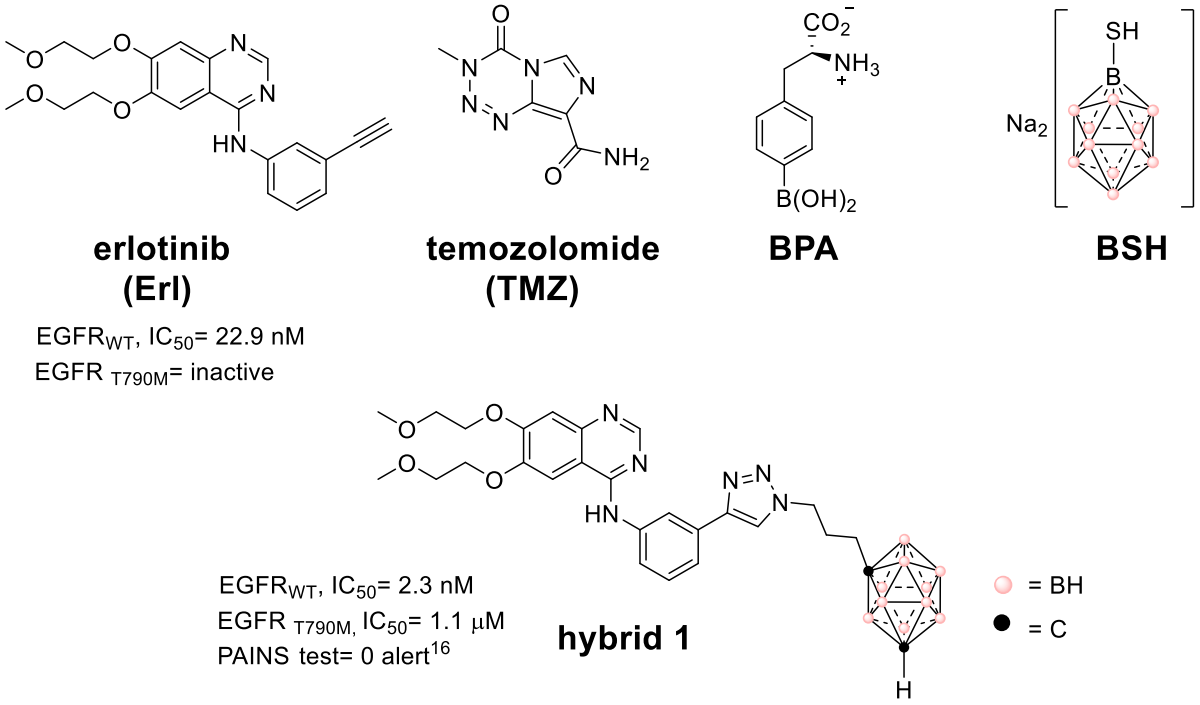

Figure 1. TKR-inhibitor **Erl**, **TMZ** used in clinical treatment of GBM. Boronated agents used in BNCT, **BPA** and **BSH**, and hybrid **1** developed in our group as bimodal therapeutic agent for glioblastoma. The Pan Assay Interference Compounds (PAINS)-filters test was performed in False Positive Remover[16].

■ MATERIAL AND METHODS

Chemistry

All chemicals were reagent grade and were used as such unless otherwise noted. **Erl**, **TMZ** and ^{10}B-**BPA-f** (99 % ^{10}B enriched, L-isomer) were acquired from Baoji Guokang Bio-Technology Co.-Ltd., Sigma and INTERPHARMA PRAHA, respectively. Solvents for synthesis were distilled and dried prior to use. Thin-layer chromatography was carried out on silica gel plates (Merck 60 F254). Column chromatography was performed on silica gel (Merck, 60–230 mesh). Hybrid **1** was prepared as previously described.[14] Modified-liposomes were prepared as previously described.[18,19]

Biology

Human glioblastoma cell line U87 MG (ATCC HTB-14) was purchased from ATCC culture collection (Virginia City, NV, USA). They were incubated in Dulbecco Modified Eagle's Medium High Glucose (4.5 g/L) with Stable Glutamine (3.97 mM) (DMEM) supplemented with 10 % heat-inactivated fetal bovine serum (i-FBS) and 1 % of a solution containing penicillin-streptomycin (PS-B) at 37 °C in a humid atmosphere containing 5 % CO_2 concentration. Culturing materials were purchased from Capricorn Scientific. In order to obtain i-FBS, original FBS was heated at 60 °C for 30 min.

Astrocytes were isolated from newborn mice. The 3-4 newborn mice were terminally anesthetized, the cerebral cortexes were dissected with the meninges previously removed. Cerebral cortexes were mechanically chopped then enzymatically dissociated using 0.25 % trypsin for 10 minutes at 37 °C. To halt trypsin digestion a mix of DMEM with FBS 10 % was added. Repetitive pipetting thoroughly disaggregated the tissue, which was then strained through an 80 μm mesh and spun down. The pellet was re-suspended in glia culture milieu and plated in T25 culture flasks. Glia culture milieu composition is as follows: DMEM supplemented with 10 % FBS, HEPES buffer (3.6 g/mL), penicillin (100 IU/mL), and streptomycin (100 μg/mL). Culture milieu was replaced every 48 h until 90 % confluence was reached.

Confocal microscopy of treated co-cultures of U87 MG and astrocytes

Astrocytes (3×10^4 cells) were seeded into p35 dishes and were allowed to grow until 80 % confluence.[14] Next, 5×10^4 U87 MG stained cells with PKH26 dye were seeded onto a

p35 dish containing a growing primary cell culture of astrocytes. After a 48 h-incubation in fresh growing milieu, the p60 dishes were treated with the $IC_{50,U87}$ doses of hybrid **1**. A p60 dish treated with 1 % DMSO served as a negative control. Treated cells were incubated for further 24 or 48 h. After that, treated co-cultures were fixed for 20 min at 4 ºC with PFA and washed 2 times with PBS. Then, samples were permeabilized for 10 min at room temperature with 0.1 % Triton X-100 in PBS, passed through washing PBS, blocked with 5 % BSA:PBS for 1 h at room temperature, and incubated overnight in a solution of 1 % BSA:PBS containing the primary antibodies and DAPI at 4 ºC. After washing, treated cells were incubated in 1:500-diluted secondary antibody during 2 h at room temperature. The following antibodies were used for immunofluorescence staining: primary antibodies 1:400 mouse monoclonal anti-GFAP (G3893, Sigma, Darmstadt, Germany) and 1:50 rat monoclonal anti-M2 (12C6c, DSHB, Iowa, United States of America) and secondary antibodies conjugated to AlexaFluor 633 AlexaFluor 488 (Invitrogen, Carlsbad, CA, USA), respectively. DAPI was used at a 1:1000 dilution. Antibodies were detected by confocal microscopy using a laser scanning Zeiss LSM 800 or LSM 880 confocal microscope.

Cellular death mechanism studies

Astrocytes (6×10^4 cells) were seeded into p60 dishes and were allowed to grow until 80 % confluence.[14] Next, 1×10^5 U87 MG stained cells with PKH26 dye were seeded onto a p60 dish containing a growing primary cell culture of astrocytes. After a 48 h-incubation in fresh growing milieu, the p60 dishes were treated with the $IC_{50,U87}$ doses of hybrid **1** or **Erl**. A p60 dish treated with 1 % DMSO served as a negative control. Treated cells were incubated for further 48 h. Then, cells were harvested with trypsin (0.05 %, supplemented with EDTA, 0.38 mg/mL), and centrifuged at 250 g speed. The resulting pellet was resuspended in an appropriate volume of Annexin binding buffer (0.01M Hepes pH 7.4, 0.14 M NaCl, and 2.5 mM $CaCl_2$) as to get a cell suspension of 1×10^6 cells per mL. After cell counts, samples were divided and cells alone and isotype-matched control samples were generated to control for nonspecific binding of antibodies and for autofluorescence. An Annexin V-FITC antibody solution (catalog number: A13199) was used at a 1:20 concentration. After 30 min of incubation with the aforementioned antibody at 4 ºC, samples were incubated with DAPI at a 1:5000 concentration and immediately after were submitted to flow cytometry analysis. To perform the analysis, cells were first gated for PKH26 in order to tell apart U87 MG cells from astrocytes. In each type of cells, the following markers were used to define four different populations: for living cells DAPI low, Annexin V low; for necrotic cells DAPI high, Annexin V low; for early apoptotic cells DAPI low, Annexin V high; and finally for late apoptotic cells DAPI high, Annexin V high. Samples were acquired using FACSAria Fusion flow cytometer and BD FACSDiva ™ software.

Confocal Raman microscopy experiments

U87 MG cells (1×10^4) were incubated in Eagle´s minimal essential milieu (DMEM) supplemented with fetal bovine serum (10 %) for 48 h. Then, they were treated with hybrid **1** at 70 or 140 μM in DMSO (lower than 1 %). A control without hybrid **1** and DMSO 1 % was included. After that, the milieu was discarded and the cells were washed (×5) with thermostatted PBS and with PBS (10 μL) were deposited on poly-L-lysine coated glass microscope coverslips for 1 hour drying with nitrogen and imaged using a Confocal Raman Microscopy system (WITec, Alpha 300RA). For visualization, cell samples were stimulated with a diode pumped solid-state (DPSS) laser operating at 532 nm and visualized with a Confocal Raman Microscope system.

Multivariate analysis. The Raman spectra of cells were analyzed using Project Five WITec Plus software, after cosmic ray removal and background subtraction for each spectrum. All the hyperspectral data were further analyzed being deconvoluted by the basis analysis algorithm "True Component" as implemented in Project Five WITec Plus, according to Dieing and Ibach.[20]

***In vitro* BNCT experiments**

Determination of intracellular boron by inductively coupled plasma optical emission spectroscopy (ICP−OES). Exponentially growing cells (F98, U87 MG or astrocytes) were incubated with hybrid **1** (0.1 μM, dissolved in DMSO) or ^{10}B-**BPA-f** (0.925 mM, diluting with water the stock solution to a final volume of 500 μL). The stock solution of ^{10}B-**BPA-f** was prepared at a concentration of 30 mg ^{10}B-**BPA-f** per mL (0.14 M) as follow: ^{10}B-**BPA** was combined in water with a 10 % molar excess of fructose, adjusting the pH to 9.5-10.0 with aqueous solution of NaOH, and the resulted mixture was stirred until all solids dissolved; finally the pH was readjusted to 7.4 with aqueous solution of HCl. After times of incubation (1, 2, and 4 h), the cells were washed twice with PBS 1× at 4 ºC. The pellets were digested with formic acid (500 μL). An aliquot of 250 μL was diluted to 1.0 mL with an aqueous solution containing 1μg/L of Y (0.75 mL) as internal standards. The boron uptake was measured by ICP-OES. Analytical and internal standard lines (innm) were as follows: B: 249.677and Y: 371.029. Matrix-matched standard solutions containing the internal standard elements and boron between 0.05 and 0.75 μg/L were employed for daily calibration. The other aliquot of 250 μL was dried and re-suspended in aqueous solution of NaOH (0.3 N) and total proteins determined by Lowry method. The boron amount was referred to the total proteins.

Neutron-irradiation procedures. Cells were irradiated at the thermal column of the RA-3 reactor, a 9 MW nuclear reactor located in Ezeiza (Argentina) where a highly thermalized and homogenous irradiation field is available. Thermal flux was near to $(1.0 \pm 0.1) \times 10^{10}$ neutrons cm^{-2} s^{-1}, the cadmium ratio was 4,100 for gold foils, which allows neglecting fast neutron dose; the gamma dose rate was approximately (4.1 ± 0.2) Gy h^{-1}. Total dose was obtained by adding partial doses coming from photons, nitrogen capture (a 3.5 % wt of nitrogen content is assumed) and boron capture. Before each irradiation, neutron flux at the irradiation position was checked using calibrated Rh-SPND detectors in a system that mimics the configuration that will be used (96-well plates or T_{25} flasks with no cells inside) while, simultaneously, signal from a boron-coated ionization chamber was used as a monitor. Based on this measurement, irradiation times were calculated in order to deliver a dose of 2 Gy with an estimated uncertainty of 10 %. Figure 7A shows, for each treatment, the time, the fluence and each dose component of the total physical absorbed dose of the neutron beam without and with boron. The intracellular boron concentration at the time of irradiation was assumed uniformly distributed inside and outside the cells for the dosimetric calculations.

Irradiation of hybrid 1- or ^{10}B-BPA-f-treated F98 or U87 MG cells assays. F98 or U87 MG cells were seeded at 2,500 cells/well in 96-well plates. Eight different wells were seeded per treatment. The cells were then treated with compounds doses equivalents to 1.0 or 10.0 ppm of ^{10}B of hybrid **1** (dissolved in DMSO) or ^{10}B-**BPA-f** (dissolved in water) for 1h after plating. Irradiated DMSO (5 %)- or irradiated water-treated cells and non-irradiated compound-treated cells served as controls. After this time the cells were irradiated with thermal neutrons with total fluence of $3.88 \times 10^{12} \pm 3 \times 10^{11}$ neutrons/cm^2.

Cell surviving assay. After irradiation, the milieu was changed and the cells were cultured at 37 ºC for 5 days. After 20 µL of vital dye MTT (Sigma 128, 0.5 %, w/v in PBS) were added to the culture milieu and after 4 h of incubation at 37 ºC absorbance at 540 nm was read. Results are expressed as percentage of untreated controls, dividing the absorbance of the irradiated-treated cells (with hybrid **1** in DMSO or with ^{10}B-**BPA-f** in water) over the absorbance of the irradiated DMSO- or water-treated cells.

Frequency of cell death analysis. Cell death of irradiated treated (1.0 ppm of ^{10}B)-cells was evaluated morphologically by fluorescence microscopy (Olympus BX51, 40X) at 48 h postirradiation. Briefly, cell pellets (10^6) were resuspended in 100 µL of a staining solution containing PI, DAF and Hoechst 33258 at the concentration of 0.6, 0.1 and 0.6 mg/mL, respectively. Results are expressed as percentage of living cells, apoptotic cells or necrotic cells per 200 total cells.

***In vivo* anti-glioblastoma studies**

Animals. All protocols for animal experimentation were carried out in accordance with experimentation procedures approved by Technion Institute of Technology Ethical Commission in the Use of Animal, Israel (Protocol number IL-143-10-17 Technion). All animal experimental protocols followed the principles outlined in the Declaration of Helsinki. Animals were housed in wire mesh cages at 20 ± 2 ºC with 12 h artificial light-dark cycles. The animals were fed *ad libitum* to standard pellet diet and water and were used after a minimum of 5 days acclimation to the housing conditions.

***In vitro* glioblastoma U87 MG cell growing.** Luciferase-transfected[19] glioblastoma U87 MG cells are grown in full milieu, MEM-Eagle with Fetal Cow Serum (9 %), glutamine (2 %) and Gentamycin (0.05 %) (Biological Industries, Beit Ha'emek, Israel). The cells are thawed and grown. After three days, the cells are split and grown for additional 4 more days until the injection. The culture milieu is changed every two days. To prepare the cells for injection into the mouse brain, they are counted and suspended in PBS.

Stereotactic surgery – cell injection in brain. The mice are anesthetized either by inhalation of isoflurane or injection of ketamine-xylazine mixture in physiological saline (ketamine 1 mg/mL:xylazine 20 mg/mL). Eye ointment was applied to maintain adequate moisture during the procedure. Using a sterile scalpel, a sagittal incision is preformed over the parieto-occipital bone, approximately 1 cm long. The exposed skull surface is then cleaned. Using stereotactic surgery, coordinates where the cells were injected are marked (1.5 mm right and 1.5 mm backward bregma). A volume of 3 mL containing 2.5-3.0 × 10^5 U87 MG cells is injected into a depth of 2.5 mm skull. After the cell injection wait 4 minutes until taking the syringe out.

Treatments. The experiments were carried out on 7-8 week-old immunosuppressed BALB/c female mice (17.6-18.0 g of body weight, bw) bred under specific pathogen-free conditions. At the end of experiments, they were anaesthetized with isoflurane and sacrificed by cervical dislocation. When tumors begin to develop, according to bioluminescence imaging (3rd day after cell inoculation), six mice per group were located in one cage and the treatments began the next day. Three groups of treatment were defined: i) hybrid **1**, dissolved sterile physiological saline:Tween 80 (4:1, v/v), administered at 4 mg/kg bw ip (n = 4); ii) hybrid **1**, encapsulated in modified-liposome, administered at 4 mg/kg bw ip (n = 5); iii) negative control (vehicle, sterile physiological saline:Tween 80 (4:1, v/v)) (n = 4). The female mice were treated three days a week every two days, with resting-days, for as long as the mice lived. Days of treatments after cells inoculation: 4th, 6th, 8th, 11th, 13th, 15th, 18th, 20th, 22th, 25th, etc. days.

Anti-tumor evaluation. The antitumor activity was evaluated using both the evolution of the tumor volumes and the animal survival. Tumor volumes were determined by bioluminescence imaging weekly. The bioluminescence imaging is based on the oxidation of luciferin [*d*-(-)-2-(6-hydroxy-2-benzothiazolyl)-thiazole-4-carboxylic acid] in the presence of oxygen and adenosine triphosphate. This reaction is catalyzed by the enzyme luciferase, which converts chemical energy into photons with resultant emission of light. Luciferase is present only in the injected cancer cells (that were pre transfected with plasmid encoding for the enzyme). Bioluminescence monitoring is done once a week beginning two days after cell injection until mice death. After the administration of luciferin (*d*-luciferin potassium salt, 150 mg/kg) via intraperitoneal injection, mice are anesthetized with isoflurane. Measurements were taken every minute until 24 min after luciferin injection. Regions of interest encompassing the intracranial area of signal are defined using Living Image software, and the total photons/s/sr/cm^2 (photons per second per radian per square cm) was recorded.

Statistical analysis. All results are expressed as the average of independent experiments ± SEM. Differences between populations were calculated with two-tailed Student's *t*-test. Kaplan–Meier survival curve and comparisons were performed by log-rank test. GraphPad Prism 6 was used for data analysis.

■ RESULTS AND DISCUSSION

Effect of hybrid 1 or Erl on co-cultures of tumor cells and normal astrocytes

Because the vast majority of cytotoxic drugs used for cancer therapy do not discriminate between tumor cells and normal cells, we previously studied the selectivity of hybrid **1** against C6 cell cultures derived from rat glioma and on a mixed primary glial cell culture. The results showed a selectivity glioma/healthy cells ratio greater than 3.3 times, indicating more toxicity to cancer cells than normal cells.[14] Herein, we have evaluated the biological behavior of hybrid **1** in an *in vitro* co-culture of primary astrocytes and human U87 MG cells, resembling the cellular environment of a developing brain tumor.[21] The co-culture was incubated with hybrid **1** at the corresponding $IC_{50,U87\ MG}$ dose (70 µM) during 24 h and 48 h (Figure 2). As shown in Figure 2, a significant decrease in the population of U87 MG cells labeled with the fluorescent dye PKH26, was observed after 24 h and 48 h. However, the population of astrocytes, immunostained with the astrocytic mem-

brane maker M2, was not affected by the incubation with hybrid **1** for 24 h nor 48 h. On the other hand, astrocyte activation was observed after treatment with hybrid **1**, as denoted by the upregulation of the glial fibrillary acid protein (GFAP), a typical marker of activated or reactive astrocytes after an injury or stress in the CNS.[22] This effect on primary astrocytes is very interesting and encouraging due to activated astrocytes play an important role in the tumor microenvironment, modulating GBM proliferation as well as radio- and chemoresistance. Voskuhl *et al.* described that the activated astrocytes form a scar between CNS lesions and the surrounding tissue.[23] This confinement of the injury site may play a considerable role in speeding up clinical stabilization and thereby improving patients' survival.[24] Besides, reactive astrocytes have also been shown to be involved in facilitating BBB repair. These findings, together with our previous studies, point out that the hybrid **1** behaves as an entity specifically directed against tumor cells and thus, render this molecule as a clear drug candidate.

To understand the type of cell death triggered by exposure to hybrid **1** or **Erl** of U87 MG cells co-cultured with mix of glial cells, flow cytometry analysis study was performed.[25,26] For that, cells were incubated with hybrid **1** or **Erl** for 48 h at the corresponding $IC_{50,U87\ MG}$ dose (70 μM and 63 μM, respectively). Based on simultaneous flow cytometry analysis of Annexin V-FITC and DAPI staining, the results showed that after treating cells with hybrid **1** about 90 % of the population suffered a late apoptosis cell death process in both cell types (Figure 3). In contrast, **Erl**, the parent compound, showed higher significant percentages of early apoptosis than the untreated cells (DMSO) on mixed glial cells and a higher percentage of early apoptosis on glioblastoma cells (Figure 3). On the other hand, recently, we described[27] that hybrid **1** promotes death in the non-co-cultured U87 MG cells mainly by necrosis while **Erl** promotes mainly early apoptosis. The difference observed in death-behavior of hybrid **1** and **Erl** in co-culture with respect to the observed in U87 MG cells alone, demonstrates the relevance of using an *in vitro* model that resembles the *in vivo* system as closely as possible in order to evaluate the actual operative death-mechanisms. These differential biological behaviors conducted us to study the toxicity of hybrid **1** or **Erl** on mouse neonatal astrocytes. The findings were significantly different between treatments of co-cultured or no-co-cultured astrocytes (Figure 4). For both compounds, hybrid **1** and **Erl**, no other cell death mechanism was observed different from that was observed in the control. Additionally, according to confocal microscopy findings hybrid **1** was not able to activate astrocytes in this condition.

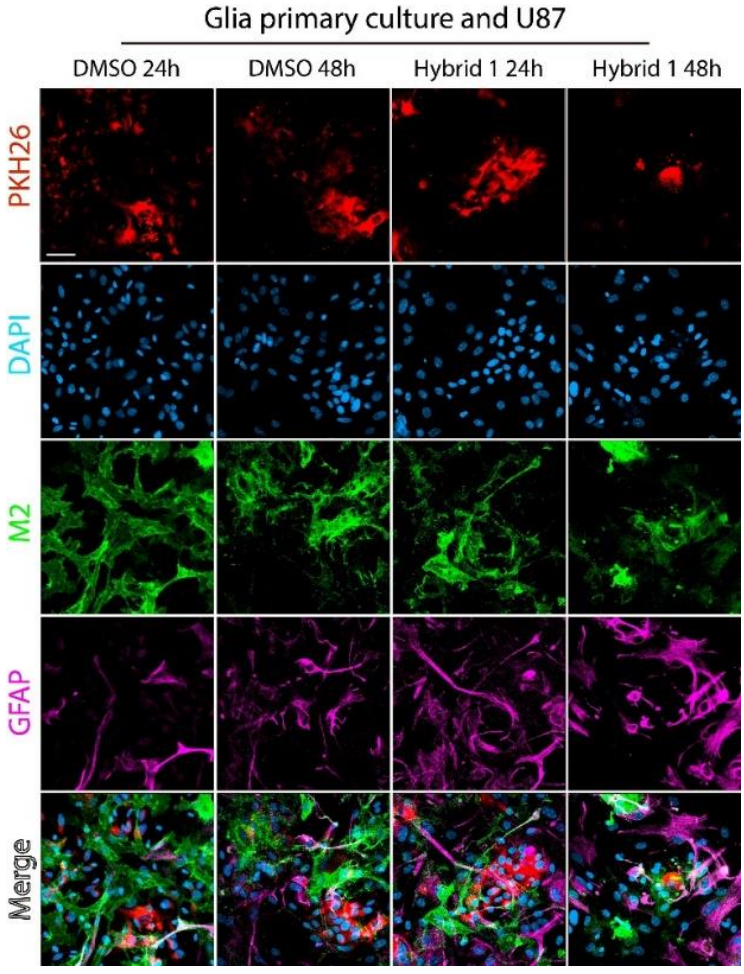

Figure 2. Effect of hybrid **1** on co-cultures cell model of astrocytes with U87 MG tumor cells. Confocal images showing the co-culture of U87 MG cells (PKH26) and mouse neonatal astrocytes (GFAP, M2). The nucleuses were stained with DAPI. Co-cultured cells were treated at $IC_{50,U87\ MG}$ doses of hybrid **1** or DMSO 1% as control for 24 and 48 h. Scale bar = 20 μm.

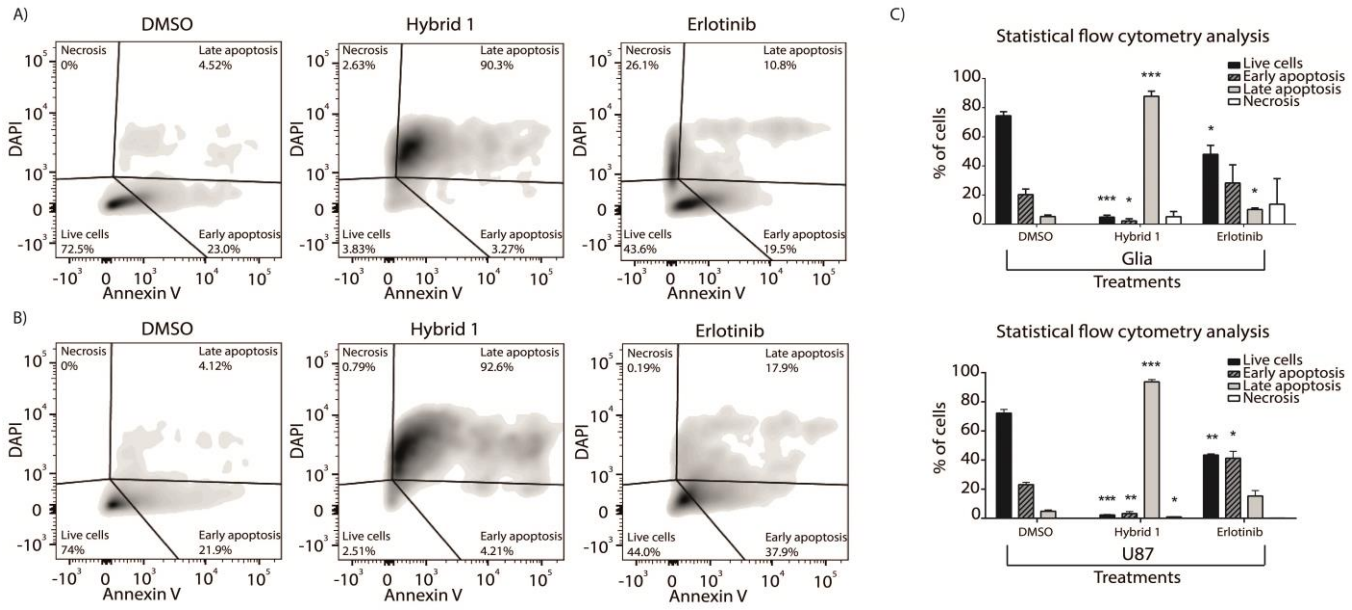

Figure 3. Phosphatidylserine exposure results for co-cultured mixed glial cells and U87 MG, panel A and B, respectively. Compound **1** and **Erl** were evaluated at their $IC_{50,U87\ MG}$ doses (70 μM and 63 μM, respectively) after incubation for 48 h. Panel **C**, quantitative analysis of flow cytometry results (three independent experiments). (*) $p < 0.05$; (**) $p < 0.01$; (***) $p < 0.001$ when compared to the negative control by Student´s *t*-test.

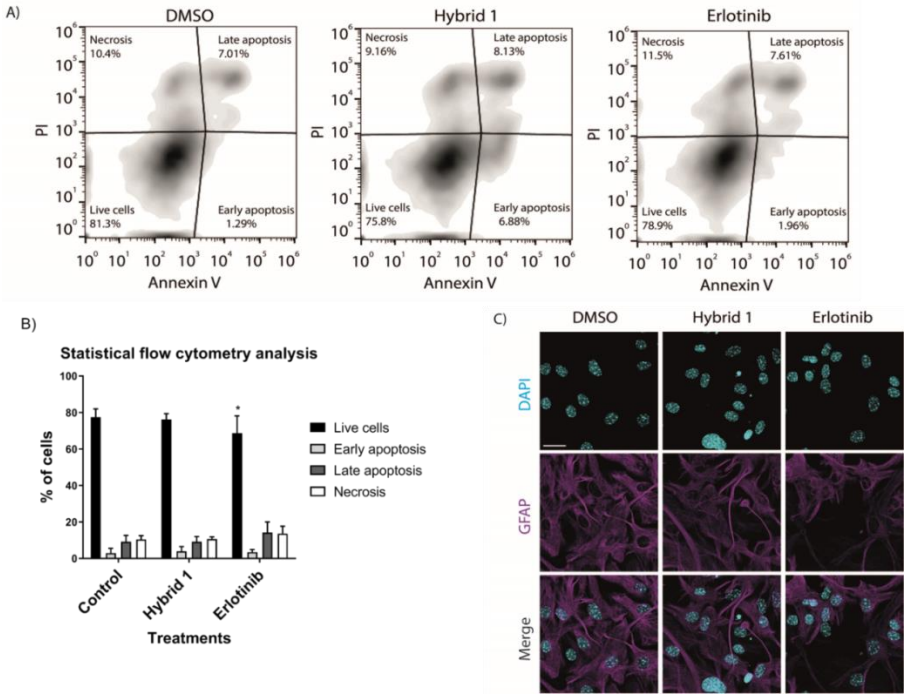

Figure 4. Panel **A**, phosphatidylserine exposure results for mixed glial cells incubated with hybrid **1** and **Erl** at their $IC_{50,U87\ MG}$ doses (70 μM and 63 μM, respectively) after incubation for 24 h. Panel **B**, quantitative analysis of flow cytometry results (three independent experiments). (*) $p < 0.05$ when compared to the negative control by Student´s *t*-test. Panel **C**, effect of hybrid **1** or **Erl** on astrocytes by confocal images (GFAP). Nuclei were stained with DAPI. The cells were treated at $IC_{50,U87\ MG}$ doses of hybrid **1**, **Erl** or DMSO 1% as control for 24 h. Scale bar = 10 μm.

Hybrid 1 uptake and localization on U87 MG cell

In the drug discovery pipeline, the distribution of drugs candidate inside cells or tissues has been investigated using different gold standard techniques such as magnetic resonance imaging, positron emission tomography, and whole body autoradiography.[28] However, some limitations, include the requirement radioisotope-labeled probes with the associated cyclotron, the use of contrast agents, low sensitivity and/or low spatial resolution, make them of limited applicability in certain cases. Although less explored technique than the above, Raman microscopy is a powerful, non-invasive, label

(radioactive or fluorescent)-free method that allows for the dynamic characterization and imaging of living biological systems, especially cells. It is a technique that can be used as a label-free marker to visualize drugs in intracellular spatial distribution of the cells if they possess bands located in the "Raman silent" region of cells (1800–2800 cm^{-1}) in which no other frequencies seen in organic molecules can be found.[29,30] In addition, affords high sensitivity to small intracellular fluctuations as well as a high spatial resolution of approximately 0.5 μm. As the ν(B-H) bonds of the carboranyl clusters appear around 2550/2630 cm^{-1}, in the "Raman silent" region of cells, carboranyl derivatives can be visualized in cells by this thecnique.[31] Thereby, as a way to know the dynamic of the internalization process of the hybrid **1** into U87 MG cells Raman microscopy experiments were performed at different time points (Figure 5).

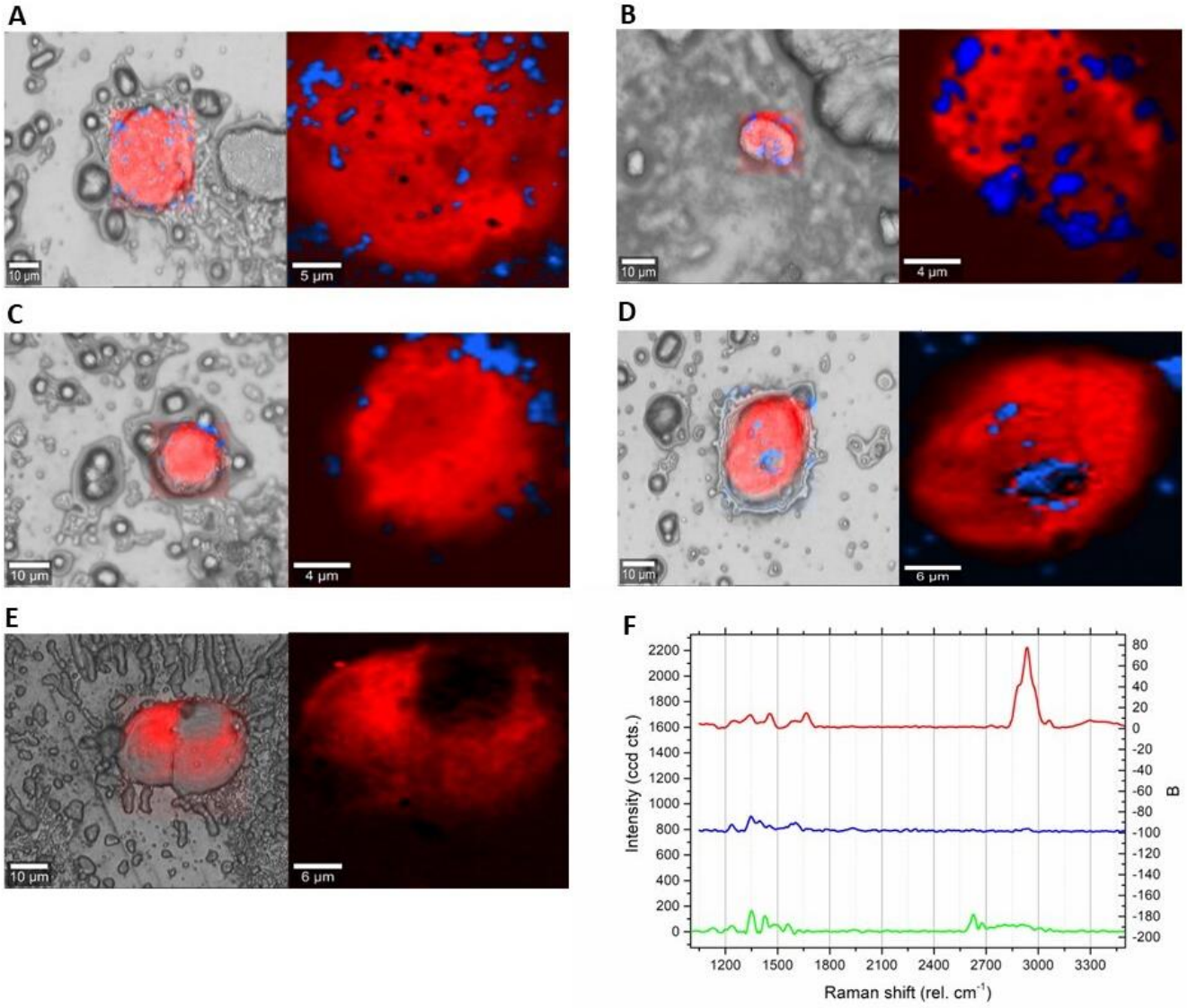

Figure 5. Panels **A-E:** White-light optical image merge with Raman image (at the left) and Raman image experiments results (at the right). Imaging of U87 MG tumor cells treated with 70 μM (panels **A** and **B**) or 140 μM of hybrid **1** (panels **C** and **D**) for 12 h of treatment (panels **A** and **C**) or 24 h of treatments (panels **B** and **D**). The scanning area corresponds to 30 × 30 $μm^2$ with 45 × 45 pixels; the laser excitation wavelength is 532 nm and the power on the samples was adjusted to 10 mW. Scale bar: 10 μm in white-light optical image and 4-6 μm in Raman image. It is shown phase contrast images superimposed to remark the B–bond Raman chemical features at 2550/2630 cm^{-1} (blue). The B–bond Raman images show hybrid **1** accumulation inside the cell. Raman spectra (panel **E**) of control cells (red), no-B-bond Raman chemical features were observed. Panel **F** shows the most representative Raman spectra, according the "True Component" Analysis for: treated cells (red), hybrid **1** within the cell (blue) and hybrid **1** as control (green).

At the hybrid **1** $IC_{50,U87\ MG}$ (70 μM) and after 12 h of incubation (Figure 5A), the boron-localization is observed at the level of the membrane and inside the cell (and in some cases outside). This could be explaining by the interaction with the EGFR, although a subsequent endocytosis process could not be ruled out. On the other hand, at 24 h (Figure 5B), the location of boron within the cell is already clear. This phenomenon is even more noticeable when we worked with $2\times IC_{50,U87\ MG}$ concentration (Figure 5C-D), observing a uniform boron-distribution in the cell periphery at shorter times and within the cell at longer times. The latter is very important when considering hybrid **1** acting as a BNCT agent because Monte Carlo simulation of the biological effect of the BNCT reaction in cells indicates that Boron accumulating in the proximity of

cell nucleus is much more efficient in cell killing than the same amount of boron uniformly distributed in the cytoplasm.[32]

Intracellular boron uptake by glioma cells treated with hybrid 1

For BNCT application, when boron atoms are located outside the cell, the physical dose delivered to the nuclei is only 10 %.[33] For this reason, the accumulation of boron atoms inside the cells is desirable to reach optimal therapeutic dose. Considering this and thinking of hybrid **1** as an antitumor agent with dual mechanism of action, targeted therapy through tyrosine kinase receptor inhibition, provoking some level of tumor cells death followed by BNCT for death of the remaining tumor cells, we determined, by inductively-coupled plasma optical emission spectrometry (ICP-OES), the accumulation of boron in normal and tumor cell lines (Figure 6A, 6B and 6C).[34,35] Normal murine astrocytes, Rattus norvegicus glioma-derived F98 cells and the U87 MG-human glioblastoma cells line were incubated for 1, 2 and 4 h, with hybrid **1** or with the BNCT-reference drug ^{10}B-**BPA-f**, both at 10 ppm of ^{10}B. Hybrid **1** showed selective accumulation on F98-glioma cells at all exposure times, reaching after 1 h and 2 h of incubation a significant glioma/astrocyte ratio of 2 (Figure 6A). On the other hand, the hybrid **1** uptake on the U87 MG cell line was very similar to that of astrocytes after 2 and 4 h of incubation (Figure 6A). Furthermore, at 2 h of exposure in both F98 and U87 MG glioma cells, boron-cellular uptake of hybrid **1** is 3-times higher than the accumulation due to ^{10}B-**BPA-f**, at the same dose of ^{10}B (10 ppm) (Figure 6B and 6C), maybe as result of the described efflux that suffers ^{10}B-**BPA-f**.[36]

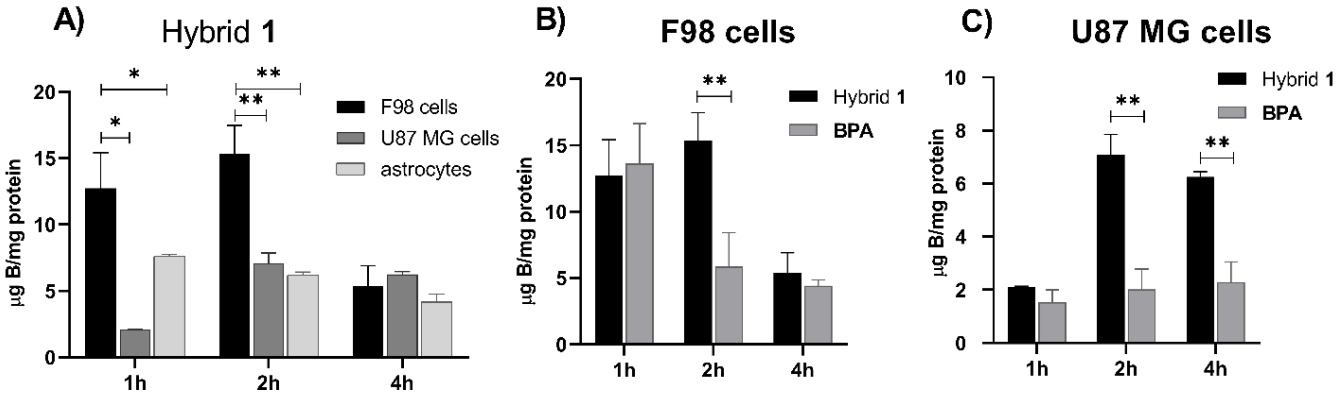

Figure 6. Amount of elemental boron incorporated into studied cells after compounds exposure. Boron concentration in F98 glioma cells, U87 MG glioma cells and astrocytes at 1, 2, and 4 h after incubation in milieu containing 10 ppm of ^{10}B from hybrid **1** (panel **A**). Boron concentration in F98 glioma cells (panel **B**) and U87 MG glioma cells (panel **C**) at 1, 2, and 4 h after incubation in milieu containing 10 ppm of ^{10}B from hybrid **1** or ^{10}B-**BPA-f**. (*) $p < 0.05$; (**) $p < 0.0001$, according to the two way Anova analysis (Tukey´s test).

***In vitro* BNCT experiments on glioma cells**

Finally, the use of hybrid **1** as a potential BNCT agent was *in vitro* studied in glioblastoma F98 and U87 MG cell lines (Figure 7).[34,35] For this, hybrid **1** or ^{10}B-**BPA-f** were incubated at an equivalent mass of 10 ppm of ^{10}B during 1 h. After this period, the plates were irradiated with a neutron flux of $(1.0 \pm 0.1) \times 10^{10}$ neutrons cm^{-2} s^{-1}, receiving a dose of 2 Gy with a fluence of 3.88×10^{12} neutrons cm^{-2} (Figure 7A). The cytotoxicity due to the capture reaction of hybrid **1** and ^{10}B-**BPA-f** upon neutron irradiation was evaluated via a MTT assay (3-(4,5-dimethylthiazol-2-yl)-2,5-diphenyltetrazolium bromide assay).[37,38] As observed in Figure 7B, ^{10}B-**BPA-f** (at a dose equivalent to 10 ppm of ^{10}B) not-significantly decreased the viability of F98 and U87 MG cell lines respect to control, while after neutron irradiation, hybrid **1** (at the identical dose of ^{10}B) provoked a significantly decrease of surviving fraction, 1.4 and 1.5-times on F98 and U87, respectively, compared to the neutron beam alone. Notably, at a physical dose of 2 Gy, the *in vitro* BNCT effect of hybrid **1** was significantly higher than ^{10}B-**BPA-f** (1.2 and 1.5-times in F98 and U87 MG, respectively). At 48 h post-neutron-irradiation with 2 Gy and at 1 ppm dose of ^{10}B, the effect of both hybrid **1** or ^{10}B-**BPA-f** on F98-cell death levels, was analyzed by fluorescence microscopy (Figure 7C). There was an increase in apoptotic cells and mitotic catastrophe in the hybrid **1**-irradiated group compared to the untreated control cells group and ^{10}B-**BPA-f**-treated group.

***In vivo* anti-glioblastoma studies of hybrid 1**

In vivo pharmacological effect of hybrid **1** was studied in immunosuppressed mouse with an intracranial xenografts tumor model derived from glioblastoma U87 MG human cells. Our preliminary data revealed that hybrid **1** exhibited relatively low aqueous solubility.[17] However, *in vitro* enhancement of anti-glioblastoma activity was achieved employing liposomes as carriers.[17] Consequently, for the *in vivo* treatments, hybrid **1** vehicularized in DMSO and in a modified-liposome were intraperitoneally administered, at 4 mg/kg/day three times a week for as long as the mice lived, using the same dosing schedule for **TMZ**, as a reference treatment, and DMSO-treatment as control (Figure 8A). Because the BBB has selective permeability and it does not allow for the entry of harmful substances such as toxins, bacteria and drugs, we previously developed a drug delivery system based on targeted-liposome[18,19] modified with a pentapeptide selected from the amyloid beta precursor protein (APP) sequence (Arg-Glu-Arg-Met-Ser). This liposomal-carrier, conjugated to 1,2-dioleoyl-sn-glycero-3-succinate-Ala-His-Arg-Glu-Arg-Met-Ser-COOH inserted in the liposomal membrane, was efficiently used as drug-delivery system.[18,19] *In vivo* tumor growth was monitored by bioluminescence of luciferase expressing U87 MG cells. When we compared, in our experiments, the median survival

of the mice group intraperitoneally administered with the hybrid **1** against the mice control group (Figure 8B), the Kaplan Meier graph showed an increase of the median survival from 25 (control) to 37 (hybrid **1**) days, which is translated to an increase by 48 % of animal survival time over control group. On the contrary, similar behavior to the control group was observed for the reference treatment with **TMZ** (average survival of 23 days)[19], which has no improvement in the median animal survival. Next, we analyzed what happened with animal survival time when hybrid **1** where given liposome-modified drug delivery system. We found out that when hybrid **1** was administered encapsulated in the modified-liposome, a notable therapeutic effect was observed with an improvement of a median survival of 51 days, increasing 100 % survival time over control. In addition, we previously found that animal treated with **TMZ**-encapsulated in this modified-liposome survived in average 39 days (62 % increase in survival time over control and the group of free **TMZ**).[18] Consequently, comparing to **TMZ**-liposome treated glioblastoma-bearing animals, the hybrid **1**–liposome provoked near to 1.3-fold increase of death-free period, from 39 to 51 days. Additionally, it was not observed toxic effects during the time of treatment (measured as evolution of the mice body weight during the assay, Figure 8C). Figure 8E shows a representative image of the bioluminescence of brain tumors undergoing different treatments. On day 21, the IVIS data collected for loaded-hybrid-**1**-treated mice was smaller than the control group (9.19×10^5 *vs*. 9.92×10^5, respectively, Figure 8D and 8E). On day 30, the effect of hybrid **1** encapsulation in targeted-liposome produced a marked decrease in luminescence compared to administration of hybrid **1**-free (9.3×10^5 *vs*. 1.26×10^6, respectively, Figure 8D). These results clearly show the remarkable *in vivo* anti-glioblastoma activity of hybrid **1**.

A)

^{10}B	Irradiation time (s)	Fluence ($\times 10^{12}$ n/cm^2)	Dose γ (Gy)	Dose ^{14}N (Gy)	Total dose without ^{10}B (Gy)	ppm ^{10}B	Dose ^{10}B (Gy)	Total dose (Gy)	Relative error dose
Without	676	3.88±0.3	0.92±0.11	1.08±0.09	2.00±0.14	0.0	0.00±0.00	2.0±0.1	±7%
With	604	3.32±0.3	0.78±0.09	0.93±0.08	1.71±0.12	1.0	0.29±0.04	2.0±0.1	±6%
With	263	1.45±0.1	0.34±0.04	0.40±0.03	0.75±0.05	10	1.3±0.2	2.0±0.2	±8%

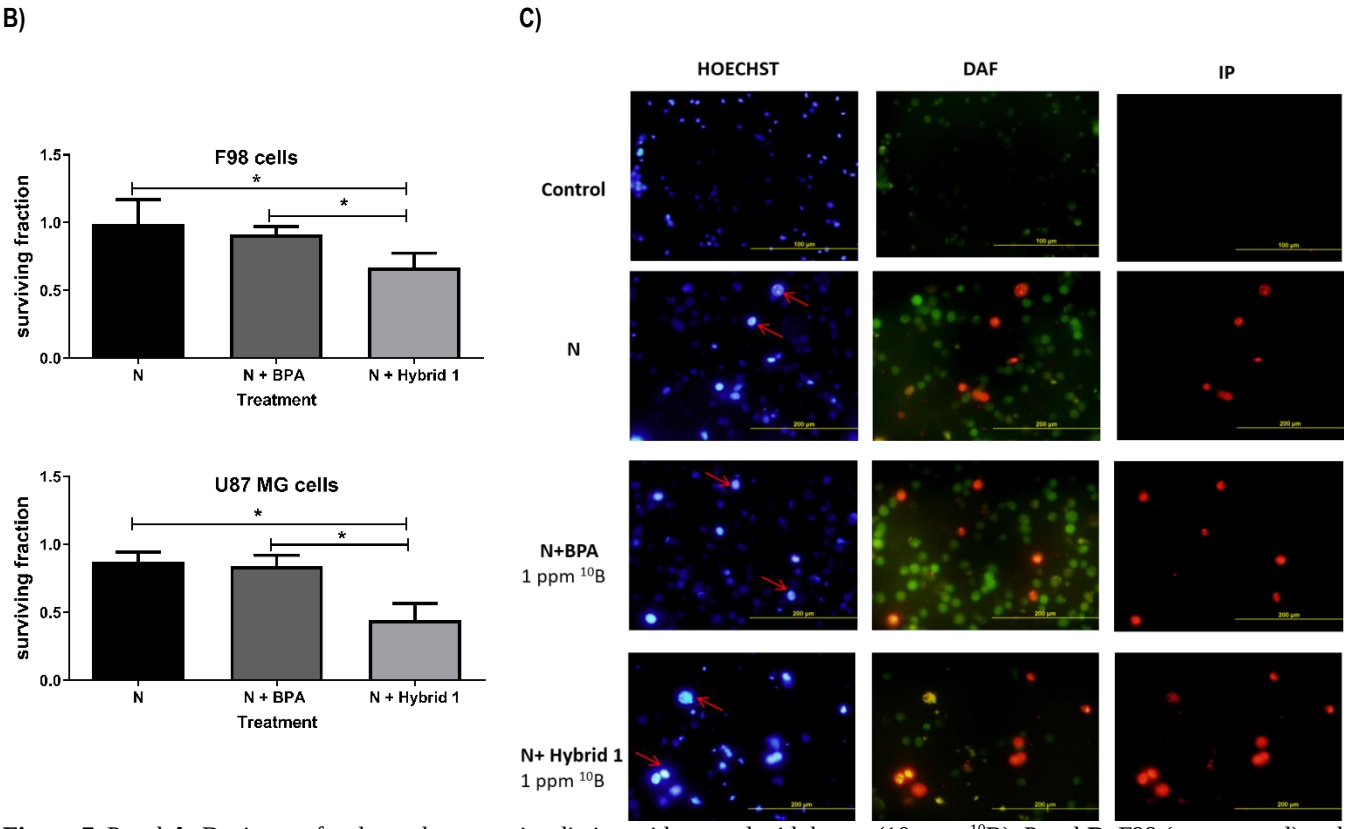

Figure 7. Panel **A**: Dosimetry for thermal neutron irradiation without and with boron (10 ppm ^{10}B). Panel **B**: F98 (upper panel) and U87 MG (lower panel) cells survival after treatment with hybrid **1** or ^{10}B-**BPA-f** (10 ppm of ^{10}B) and post neutron-irradiation (2 Gy) (BNCT *in vitro* experiments). Unpaired *t* test (*) $p < 0.05$. Panel **C**: Fluorescence microscopy analyzing apoptotic or necrotic cells post-neutron-irradiation in the different treatments. Representative images from stained cells 48 h after irradiation. Apoptotic nuclei labeled with Hoechst 33258 (red arrowheads and inset) exhibited peripheral chromatin clumping, blebbing and fragmentation; cytoplasm of living cells was labeled with 4,5-diaminofluorescein (DAF) and necrotic cells were labeled with propidium iodide (IP). Abbreviations: N= assay without compounds incubation and with neutron irradiation; N+BPA 1 ppm ^{10}B = assay with BPA incubation at a dose equivalent to 1 ppm of ^{10}B and with neutron irradiation; N+**1** 1 ppm ^{10}B = assay with hybrid **1** incubation at a dose equivalent to 1 ppm of ^{10}B and with neutron irradiation.

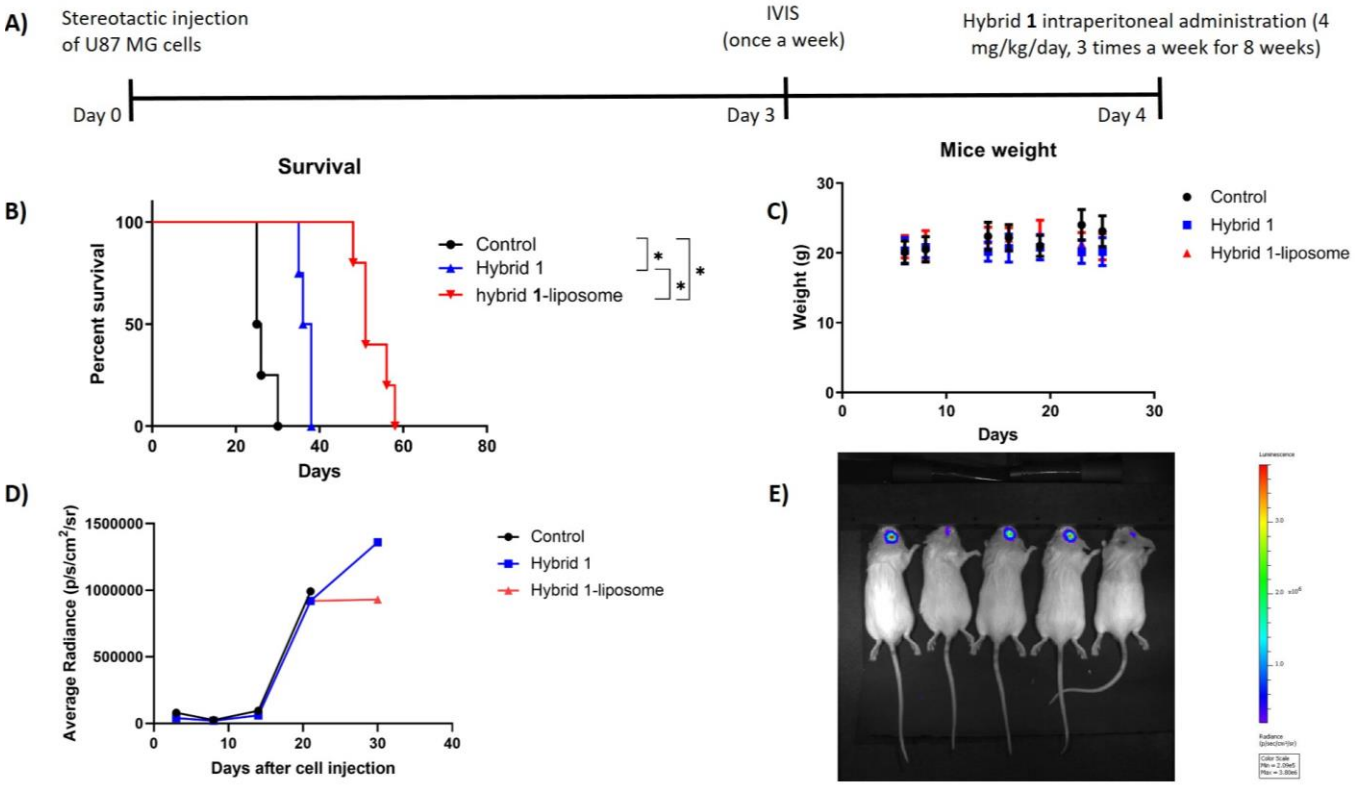

Figure 8. Panel **A**: Schedule of the *in vivo* experiments. Panel **B**: Kaplan-Meier survival curves of U87 MG glioma bearing mice. Black: control animals (n = 4); blue: hybrid **1** treated animals (n = 4); and yellow: hybrid **1**-modified liposome treated animals (n = 5). The results showed significant difference ($p < 0.01$) between: hybrid **1** *vs* control (DMSO-treated animals); hybrid **1**-modified liposome *vs* control; and hybrid **1** *vs* hybrid **1**-modified liposome. Data were analyzed by log-rank test. Panel **C**: Evolution of mice body weight during treatment. Panel **D**: Evolution of the GBM sizes during the time of treatment. Panel **E**: Selected images of the evolution of GBM sizes corresponding to 21st day.

■ CONCLUSIONS

Hybrid **1**, designed as a bimodal agent by combination of a TKR-inhibitor moiety and a boron-rich group,[39] demonstrated excellent ability to inhibit wild type EGFR, good ability to inhibit mutant $EGFR_{T790M}$ and adequate like-drug properties (absence of alert in PAINS test, absence of mutagenicity without and with metabolic activation, high oral LD_{50} and ability to be formulated using liposomes).

Herein, we describe other performed studies that allowed us to deepen our knowledge of hybrid **1** as a potential anti-glioma drug. Thus, we showed that hybrid **1** in a simulated tumor microenvironment: i) produces, unlike **Erl**, late-apoptosis cell death in astrocytes and U87 MG cells; ii) increases the activated-astrocytes population. Furthermore, according to Raman confocal microscopy, it retains **Erl** cellular-uptake mechanism.

Moreover, it was demonstrated, by ICP-OES, that hybrid **1** is an efficient and selective way to accumulate boron atoms in glioma cells, having a F98 glioma/astrocyte boron ratio of 3 after 2 h of incubation, opening, this capability, the possibility of dual therapy through boron neutron capture therapy along with TKR inhibition. It was confirmed by the *in vitro* BNCT proof of concept assay, over glioma cells, a better activity of hybrid **1**, in the same conditions of dosage and neutrons-irradiation, than ^{10}B-**BPA-f**. It should also be noted that the synthesis of hybrid **1** was carried out starting from carborane with a natural ratio of boron $^{10}B/^{11}B$ (20 % of ^{10}B and 80 % of ^{11}B isotopes), so the next step to take in our laboratory is the preparation of hybrid **1** enriched 99 % in ^{10}B.

Additionally, and one of the most significant findings of this study was that hybrid **1** and hybrid **1**-encapsulated in APP-targeted liposomal system significantly increases the median survival period of glioma-induced mice, from 1.5 (in DMSO) to 2 (in modified-liposomes) times higher than both control or therapeutic used drug **TMZ**-treated mice median survival.

Overall, these encouraging results are promising and open the way to further explore the possibility of hybrid **1** as an anti-glioma drug candidate with a bimodal mode of action.

AUTHOR INFORMATION

Corresponding Authors

Marcos Couto - Grupo de Química Orgánica Medicinal, Instituto de Química Biológica, Facultad de Ciencias, Universidad de la República, Iguá 4225, Montevideo 11400, Uruguay. E-mail: mcouto@fcien.edu.uy

Hugo Cerecetto - Área de Radiofarmacia, CIN, Facultad de Ciencias, Mataojo 2055, Montevideo 11400, Uruguay. E-mail: hcerecetto@cin.edu.uy

Moshe Gavish - Molecular Pharmacology, Faculty of Medicine, Technion Institute of Technology, Haifa 3109601, Israel. E-mail: mgavish@technion.ac.il

Authors Contributions

† These authors contributed equally.

MC and HC written the manuscript. All authors revised the final version. All authors have given approval to the final version of the manuscript.

Notes

The authors declare no competing financial interest.

ACKNOWLEDGMENTS

This research was funded by Agencia Nacional de Investigación e Innovación (ANII, Uruguay), grant numbers FCE_3_2018_1_148288 and POS_NAC_2015_1_110068, Institut Pasteur de Montevideo—FOCEM, and Comisión Sectorial de Investigación Científica-Universidad de la República (Uruguay). M.F.G., E.T., R.F., H.C. and M.C. are Sistema Nacional de Investigadores-ANII researchers.

ABBREVIATIONS USED

BBB - Blood-brain barrier

BNCT – Boron Neutron Capture Therapy

BPA - Boronophenylalanine

BPA-f - Boronophenylalanine fructose adduct

BSH - mercaptoundecahydro-*closo*-dodecaborate or sodium borocaptate

CNS - Central Nervous System

DAF - 4,5-Diaminofluorescein

DMSO - Dimethylsulfoxide

EGFR - Epidermal growth factor receptor

Erl - Erlotinib

GBM - Glioblastoma

GFAP - Glial fibrillary acid protein

IC_{50} - Half maximal inhibitory concentration

ICP-OES - Jnductively-coupled plasma optical emission spectrometry

IP - Propidium iodide

MTT - 3-(4,5-Dimethylthiazol-2-yl)-2,5-diphenyl tetrazolium bromide

PAINS - Pan-assay interference compounds

PBS - Phosphate-buffered saline

TKR - Tyrosine Kinase Receptors

TMZ - Temozolomide

REFERENCES

(1) Fitzmaurice, C.; Dicker, D.; Pain, A. *et al.* The global burden of cancer 2013. *JAMA Oncol.* **2015**, *1*, 505-527. DOI: 10.1001/jamaoncol.2015.0735.

(2) Taylor, O. G.; Brzozowski, J. S.; Skelding, K. A. Gliobastoma multiforme: An overview of emerging therapeutic targets. *Front. Oncol.* **2019**, *9*, 963. DOI: 10.3389/fonc.2019.00963.

(3) Kim, G.; Tag Ko, Y. Small molecule tyrosine kinase inhibitors in glioblastoma. *Arch. Pharm. Res.* **2020**, *43*, 385-394. DOI: 10.1007/s12272-020-01232-3.

(4) Lombardi, G.; Caccese, M.; Padovan, M.; Cerretti, G.; Pintacuda, G.; Manara, R.; Di Sarra, F.; Zagonel, V. Regorafenib in recurrent glioblastoma patients: A large and monocentric real-life study. *Cancers (Basel).* **2021**, *13*, 4731. DOI: 10.3390/cancers13184731.

(5) Aldaz, P.; Arozarena, I. Tyrosine kinase inhibitors in adult glioblastoma: An (un)closed chapter? *Cancers (Basel).* **2021**, *13*, 5799. DOI: 10.3390/cancers13225799.

(6) Wang, Q.; Niu, W.; Pan, H. Targeted therapy with anlotinib for a H3K27M mutation diffuse middle glioma patient with PDGFR-alpha mutation: A case report. *Acta Neurochir. (Wien).* **2021**, 1-4. DOI: 10.1007/s00701-021-05061-1.

(7) Chen, H.; Kuhn, J.; Lamborn, K. R.; Abrey, L. E.; DeAngelis, L. M.; Lieberman, F.; Robins, H. I.; Chang, S. M.; Yung, W. K. A.; Drappatz, J.; Mehta, M. P.; Levin, V. A.; Aldape, K.; Dancey, J. E.; Wright, J. J.; Prados, M. D.; Cloughesy, T. F.; Wen, P. Y.; Gilbert, M. R. Phase I/II study of sorafenib in combination with erlotinib for recurrent glioblastoma as part of a 3-arm sequential accrual clinical trial: NABTC 05-02. *Neurooncol. Adv.* **2020**, *2*, vdaa124. DOI: 10.1093/noajnl/vdaa124.

(8) D´alessandris, Q. G.; Martini, M.; Cenci, T.; Di Bonaventura, R.; Lauretti, L.; Stumpo, V.; Olivi, A.; Larocca, L. M.; Pallini, R.; Montano, N. Tailored therapy for recurrent glioblastoma. Report of a personalized molecular approach. *J. Neurosurg. Sci.* **2020**. DOI: 10.23736/S0390-5616.20.04943-7. DOI: 10.23736/S0390-5616.20.04943-7.

(9) Prados, M.; Chang, S.; Butowski, N.; DeBoer, R.; Parvataneni, R.; Carliner, H.; Kabuubi, P.; Ayers-Ringler, J.; Rabbitt, J.; Page, M.; Fedoroff, A.; Sneed, P. K.; Berger, M. S.; McDermott, M. W.; Parsa, A. T.; Vandenberg, S.; James, C. D.; Lamborn, K. R.; Stokoe, D.; Hass-Kogan, D. A. Phase II study of erlotinib plus temozolomide during and after radiation therapy in patients with newly diagnosed glioblastoma multiforme or gliosarcoma. *J Clin Oncol.* **2009**, *27*, 579-584. DOI: 10.1200/JCO.2008.18.9639.

(10) Yan, G.; Wang, Y.; Chen, J.; Zheng, W.; Liu, C.; Chen, S.; Wang, L.; Luo, J.; Li, Z. Advances in drug development for targeted therapies for glioblastoma. *Med. Res. Rev.*, **2020**, *40*, 1950-1972. DOI: 10.1002/med.21676.

(11) Cerecetto, H.; Couto, M. Medicinal Chemistry of Boron-Bearing Compounds for BNCT in Glioma Treatment: Current Challenges and Perspectives in Glioma Contemporary Diagnostic and Therapeutic Approaches; I. Omerhodzic and K. Arnautovic, Eds; IntechOpen Ltd., United Kingdom, 2018. DOI: 10.5772/intechopen.76369.

(12) Barth, R.; Mi, P.; Yang, W. Boron delivery agents for neutron capture therapy of cancer. *Cancer Commun.* **2018**, *38*, 35. DOI: 10.1186/s40880-018-0299-7.

(13) Goodman, J. H.; Yang, W.; Barth, R. F.; Gao, Z.; Boesel, C. P.; Staubus, A. E.; Gupta, N.; Gahbauer, R. A.; Adams, D. M.; Gibson, C. R.; Ferketich, A. K.; Moeschberger, M. L.; Soloway, A. H.; Carpenter, D. E.; Albertson, B. J.; Bauer, W. F.; Zhi Zhang, M.; Cheng Wang, C. Boron neutron capture therapy of brain tumors: Biodistribution, pharmacokinetics, and radiation dosimetry of sodium borocaptate in patients with gliomas. *Neurosurgery* **2000**, *47*, 608-622. DOI: 10.1097/00006123-200009000-00016.

(14) Couto, M.; Mastandrea, I.; Cabrera, M.; Cabral, P.; Teixidor, F.; Cerecetto, H.; Viñas, C. Small-molecule kinase-inhibitors-loaded boron cluster as hybrid agents for glioma-cell-targeting therapy. *Chem. Eur. J.* **2017**, *23*, 9233-9238. DOI: 10.1002/chem.201701965.

(15) Couto, M.; García, M. F.; Alamón, C.; Cabrera, M.; Cabral, P.; Merlino, A.; Teixidor, F.; Cerecetto, H.; Viñas, C.

Discovery of potent EGFR inhibitors through the incorporation of a 3D-aromatic-boron-rich-cluster into the 4-anilinoquinazoline scaffold: Potential drugs for glioma treatment. *Chem. Eur. J.* **2018**, *24*, 3122-3126. DOI: 10.1002/chem.201705181.

(16) Xie, X. Q. URL: https://www.cbligand.org/PAINS/. (accessed 2022-12-05).

(17) Couto, M.; Alamón, C.; Sánchez, C.; Dávila, B.; Fernández, M.; Lecot, N.; Cabral, P.; Teixidor, F.; Viñas, C.; Cerecetto, H. Carboranylanilinoquinazoline EGFR-inhibitors: Toward "lead-to-candidate" stage in the drug-development pipeline. *Fut. Med. Chem.* **2019**, *11*, 2273-2285. DOI: 10.4155/fmc-2019-0060.

(18) Kahana, M.; Weizman, A.; Gabay, M.; Loboda, Y.; Segal-Gavish, H.; Gavish, A.; Barhum, Y.; Offen, D.; Finberg, J.; Allon, N.; Gavish, M. Liposome-based targeting of dopamine to the brain: a novel approach for the treatment of Parkinson's disease. *Mol. Psychiatry*. **2021**, *26*, 2626-2632. DOI: 10.1038/s41380-020-0742-4.

(19) Gabay, M.; Weizman, A.; Zeineh, N.; Kahana, M.; Obeid, F.; Allon, N-: Gavish, M. Liposomal carrier conjugated to APP-derived peptide for brain cancer treatment. *Cell Mol. Neurobiol*. **2021**, *41*, 1019-1029. DOI: 10.1007/s10571-020-00969-1.

(20) Dieing, T.; Ibach W. Software Requirements and Data Analysis in Confocal Raman Microscopy in Confocal Raman Microscopy; T. Dieing, O. Hollricher and J. Toporski, Eds; Springer Series in Optical Sciences, vol 158. Springer, Berlin, Heidelberg, 2010. DOI 10.1007/978-3-642-12522-5.

(21) Civita, P.; M. Leite, D.; Pilkington, G.J. Pre-Clinical Drug Testing in 2D and 3D Human In Vitro Models of Glioblastoma Incorporating Non-Neoplastic Astrocytes: Tunneling Nano Tubules and Mitochondrial Transfer Modulates Cell Behavior and Therapeutic Response. *Int. J. Mol. Sci.* **2019**, *20*, 6017. DOI: 10.3390/ijms20236017.

(22) Kawata, K.; Tierney, R.; Langford, D. Blood and cerebrospinal fluid biomarkers in Handbook of Clinical Neurology; Hainline, B and Stern, R, Eds; Elsevier, 2018. DOI: 10.1016/B978-0-444-63954-7.00022-7.

(23) Voskuhl, R. R.; Peterson, R. S.; Song, B.; Ao, Y.; Morales, L. B. J.; Tiwari-Woodruff, S.; Sofroniew, M. V. Reactive astrocytes form scar-like perivascular barriers to leukocytes during adaptive immune inflammation of the CNS. *J. Neutrosci.* **2009**, *29*, 11511-11522. DOI: 10.1523/JNEUROSCI.1514-09.2009.

(24) Cregg, J. M.; DePaul, M. A.; Filous, A. R.; Lang, B. T.; Tran, A.; Silver, J. Functional regeneration beyond the glial scar. *Exp. Neurol.* **2014**, *253*, 197-207. DOI: 10.1016/j.expneurol.2013.12.024.

(25) Biegański, P.; Godel, M.; Riganti, C.; Kawano, D. F.; Kopecka, J.; Kowalski, K. Click ferrocenyl-erlotinib conjugates active against erlotinib-resistant non-small cell lung cancer cells in vitro. *Bioorg. Chem.* **2021**, *119*, 105514. DOI: 10.1016/j.bioorg.2021.105514.

(26) Alamón, C.; Dávila, B.; García, M. F.; Sánchez, C.; Kovacs, M.; Trias, E.; Barbeito, L.; Gabay, M.; Zeineh, N.; Gavish, M.; Teixidor, F.; Viñas, C.; Couto, M.; Cerecetto, H. Sunitinib-containing carborane pharmacophore with the ability to inhibit tyrosine kinases receptors FLT3, KIT and PDGFR-β, exhibits powerful *in vivo* anti-glioblastoma activity. *Cancers (Basel).* **2020**, *12*, 3423. DOI: 10.3390/cancers12113423.

(27) Alamón, C.; Dávila, B.; Cerecetto, H.; Couto, M. Exploring the cell death mechanism of cytotoxic [1,2,3]triazolylcarborane lead compounds against U87 MG human glioblastoma cells. *Chem. Biol. Drug Des.* **2023**. DOI: 10.1111/cbdd.14208.

(28) Mudd, S. R.; Comley, R. A.; Bergstrom, M.; Holen, K. D.; Luo, Y.; Carme, S.; Fox, G. B.; Martarello, L.; Beaver, J. D. Molecular imaging in oncology drug development. *Drug Discov. Today.* **2017**, *22*, 140-147. DOI: 10.1016/j.drudis.2016.09.020.

(29) Meister, K.; Niesel, J.; Schatzschneider, U.; Metzler-Nolte, N.; Schmidt, D. A.; Havenith, M. Raman Microspectroscopic Evidence for the Metabolism of a Tyrosine Kinase Inhibitor, Neratinib, in Cancer Cells. *Angew. Chem. Int. Ed.* **2010**, 122, 3382-3384. DOI: 10.1002/anie.201803394.

(30) Hildebrandt, P. A Spectral Window to the Cell. *Angew. Chem. Int. Ed*. **2010**, 49, 4540-4541. DOI: 10.1002/anie.201001616.

(31) Tarrés, M.; Canetta, E.; Viñas, C.; Teixidor, F.; Harwood, A. J. Imaging in living cells using νB–H Raman spectroscopy: monitoring COSAN uptake. *Chem. Commun.* **2014**, *50*, 3370-3372. DOI: 10.1039/C3CC49658A.

(32) Gabel, D.; Foster, S.; Fairchild, R. G. The Monte Carlo simulation of the biological effect of the ^{10}B(n, alpha)^{7}Li reaction in cells and tissue and its implication for boron neutron capture therapy. *Radiat. Res*. **1987**, 111, 14-25. DOI: 10.2307/3577018.

(33) Revell, S.H. Relationship between chromosome damage and cell death. In Ishihara, T.; Sasaki, M. S., editors: Radiation-induced chromosome damage in man. New York: Alan R. Liss, Inc.; 1983. pp. 215–233.

(34) Couto, M.; Alamón, C.; Nievas, S.; Perona, M.; Dagrosa, M. A.; Teixidor. F.; Cabral, P.; Viñas, C.; Cerecetto, H. Bimodal therapeutic agents against glioblastoma, one of the most lethal forms of cancer. *Chem. Eur. J.* **2020**, *26*, 14335-14340. DOI: 10.1002/chem.202002963.

(35) Couto, M.; Alamón, C.; García, M. F.; Kovacs, M.; Trias, E.; Nievas, S.; Pozzi, E.; Curotto, P.; Thorp, S.; Dagrosa, M. A.; Teixidor. F.; Viñas, C.; Cerecetto, H. *Closo*-carboranyl- and metallacarboranyl [1,2,3]triazolyl-decorated Lapatinib-scaffold for cancer therapy combining tyrosine kinase inhibition and boron neutron capture therapy. *Cells*. **2020**, *9*, 1408. DOI: 10.3390/cells9061408.

(36) Nomoto, T.; Inoue, Y.; Yao, Y.; Suzuki, M.; Kanamori, K.; Takemoto, H.; Matsui, M.; Tomoda, K.; Nishiyama, N. Poly(vinyl alcohol) boosting therapeutic potential of *p*-boronophenylalanine in neutron capture therapy by modulating metabolism. *Sci. Adv.* **2020**, *6*, eaaz1722. DOI: 10.1126/sciadv.aaz1722.

(37) Dagrosa, M. A.; Crivello, M.; Perona, M.; Thorp, S.; Santa Cruz, G. A.; Pozzi, E.; Casal, M.; Thomasz, L.; Cabrini, R.; Kahl, S.; Juvenal, G. J.; Pisarev, M. A. First evaluation of the biologic effectiveness factors of boron neutron capture therapy (BNCT) in a human colon carcinoma cell line. *Int. J. Radiat. Oncol. Biol. Physics.* **2011**, *79*, 262-268. DOI: 10.1016/j.ijrobp.2010.07.020.

(38) Perona, M.; Pontiggia, O.; Carpano, M.; Thomasz, L.; Thorp, S.; Pozzi, E.; Simian, M.; Kahl, S.; Juvenal, G.;

Pisarev, M.; Dagrosa, A. *In vitro* studies of cellular response to DNA damage induced by boron neutron capture therapy. *Appl. Radiat. Isot.* **2011**, *69*, 1732-1736. DOI: 10.1016/j.apradiso.2011.03.044.

(39) Marfavi, A.; Kavianpour, P.; Rendina, L.M. Carboranes in drug discovery, chemical biology and molecular imaging. *Nat. Rev. Chem.* **2022**, *6*, 486-504. DOI:10.1038/s41570-022-00400-x.

For Table of Contents Graphic Use Only

A Potential BNCT Agent Selectively Suppresses High-Grade Glioma: In Vitro and In Vivo Exploration

Catalina Alamón, Belén Dávila María Fernanda García, Susana Nievas, María Alejandra Dagrosa, Silvia Thorp, Mariángeles Kovacs, Emiliano Trias, Ricardo Faccio, Martín Gabay, Nidal Zeineh, Abraham Weizman, Francesc Teixidor, Clara Viñas, Moshe Gavish, Hugo Cerecetto, Marcos Couto

The boron-rich EGFR-inhibitor **1**, with good drug-like properties, is potential BNCT- and a potent *in vivo* anti-glioblastoma-agent.

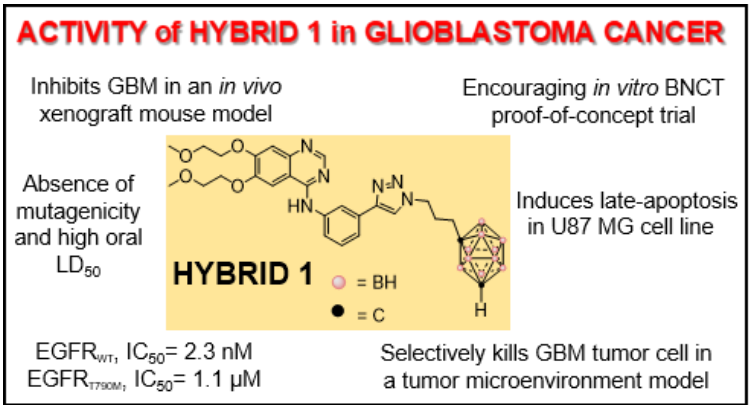

Table of Contents